Virus-Mimetic Gene Transfer

DOI: 10.1002/ange.201301113

Virus-Mimetic Cytoplasm-Cleavable Magnetic/Silica Nanoclusters for Enhanced Gene Delivery to Mesenchymal Stem Cells**

*Naveen Gandra, Dong-Dong Wang, Ye Zhu, and Chuanbin Mao**

Development of non-viral gene delivery vectors for transfecting mesenchymal stem cells (MSCs) will advance tissue engineering and regenerative medicine to treat several health disparities associated with the heart, brain, spinal cord, bone, and blood vessels.[1] In the last decade, there has been remarkable progress in regenerative medicine using stem cells for therapeutic applications.[2] However, to use these cells more effectively, enabling them to express functional proteins is crucial for rapid formation and repair of tissues and organs. For example, vascular endothelial growth factor (VEGF) is essential for angiogenesis for the progression of new blood vessels. Indeed, efficient VEGF gene expression in MSCs can stimulate the formation of new blood vessels. However, the transfection of VEGF gene into stem cells is difficult and challenging because stem cells are hard to transfect. To date, the most efficient gene delivery vectors used in MSCs are genetically engineered viruses encompassing a gene of interest.[3] The major limitations in using viral vectors are their inherent toxicity and ability to induce immune and inflammatory responses. This fact drives research on the development of biocompatible non-viral vectors such as cationic lipids, polymers, hydrogels, and synthetic nanoparticles (NPs).[4] But these non-viral vectors are less effective when compared with viral vectors, which is mainly due to the lack of efficient homing and internalization capability of foreign genes. When nonviral vectors, such as liposomes, chitosan, or polyethyleneimine (PEI), are used to transfect stem cells, the transfection efficiency is usually low.[5] Therefore, there is an urgent need in regenerative medicine to develop safe and efficient non-viral vectors for delivering a foreign gene to MSCs.

We have now demonstrated the virus mimetic magnetic silica nanoclusters (VMSNCs) for gene delivery to rat MSCs (Figure 1). The VMSNCs are designed on the following observations. First, fd-tet phage is a virus that specifically infects bacteria by transferring DNA to host cells and is nontoxic to human beings. It is made of DNA encapsulated by a protein coat (Figure 1). The protein coat includes about 3900 copies of major coat protein (pVIII) on the side wall of phage and about 5 copies each of four minor coat proteins at the two tips of the phage.[6] We have recently used the phage display technique to discover fd-tet phage particles that display a MSC-targeting peptide (VTAMEPGQ) as fusion to each pVIII constituting the side wall of phage.[7] We also found that the MSC-targeting peptide could promote the delivery of the gene into MSCs once presented on liposome NPs.[7] Second, embedding superparamagnetic iron oxide (SPIO) NPs in a silica matrix can aid magnetically guided gene delivery, which is crucial for future in vivo applications. Third, the porous structure formed owing to the aggregation of SPIO and silica NPs in the nanoclusters through S–S bonds (Figure 2 and Scheme 1) can safely hold and protect DNA before gene release and expression. Fourth, pVIII can be purified from fd-tet phage body,[8] thus MSC-targeting pVIII

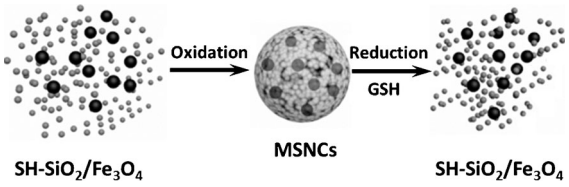

Scheme 1. Mechanism of magnetic/silica nanocluster (MSNC) formation and their subsequent cleavage. Fe_3O_4 NPs are embedded inside a porous matrix aggregated from silica NPs through the S–S bond. The resultant cluster is porous and can hold loaded DNA. In the presence of intracellular GSH, the S–S bond will be broken to dissociate the clusters, favoring the release of gene loaded in the porous silica matrix.

can be purified and then chemically conjugated with PEI to ensure the targeting of the cluster to MSCs after PEI is conjugated with the surface of the cluster to protect DNA. Last, once the cluster is internalized in the MSCs, the S–S bonds holding the NPs together in the cluster can be cleaved by intracellular glutathione (GSH; Scheme 1) to make the cluster dissociated, leading to the DNA release and expression for improved gene transfection. The VMSNCs mimic phage structure by bearing phage-borne pVIII on the surface and loading DNA inside, promoting their cell-internalization and transferring gene to MSCs.

[*] N. Gandra,[+] D. Wang,[+] Y. Zhu, Prof. C. B. Mao
Department of Chemistry & Biochemistry
Stephenson Life Sciences Research Center
University of Oklahoma, 101 Stephenson Parkway, Room 3310
Norman, OK 73019-5300 (USA)
E-mail: cbmao@ou.edu

[+] These authors contributed equally to this work.

[**] We would like to thank the National Science Foundation (CBET-0854465, CBET-0854414 and DMR-0847758), National Institutes of Health (4R03AR056848-03, 1R21EB015190-02, and 5R01HL092526-02), Department of Defense Peer Reviewed Medical Research Program (W81XWH-12-1-0384), Oklahoma Center for the Advancement of Science and Technology (HR11-006), and Oklahoma Center for Adult Stem Cell Research (434003) for their generous financial support. We also want to thank Dr. Haibao Zhu and Dr. Gopal Abbineni for their kind help during experiments.

Supporting information for this article is available on the WWW under http://dx.doi.org/10.1002/anie.201301113.

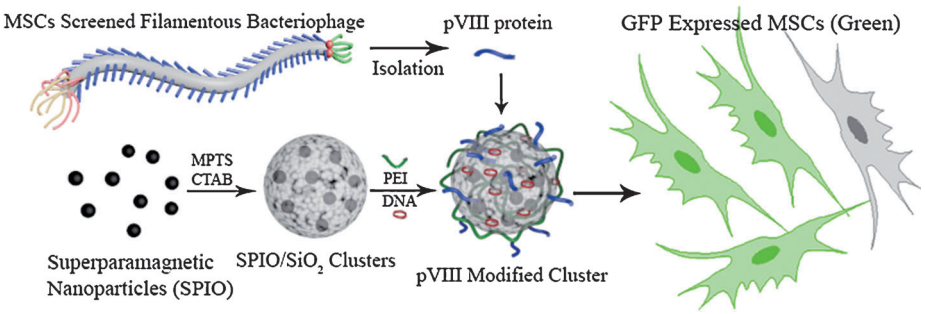

Figure 1. VMSNCs for gene delivery to MSCs. The MSC-targeting phage particle has about 3900 copies of pVIII with the MSC-targeting peptide fused to the solvent-exposed terminal. The MSC-targeting pVIII can be isolated and purified from the phage. Cleavable magnetic/silica nanoclusters (MSNCs) are synthesized by embedding SPIO NPs in the silica network, which is achieved by in situ hydrolysis of tetraethyl orthosilicate (TEOS) and (3-mercaptopropyl)trimethoxysilane (MPTS) in the presence of SPIO NPs dispersed in cetyl trimethylammonium bromide (CTAB). Then the DNA (red circles) is incorporated into the porous structure of the SPIO-embedded silica matrix. The MSNCs are then modified with PEI, which is conjugated with pVIII (blue) purified from MSC-targeting phage by EDC/NHS chemistry, to form VMSNCs. Bearing phage-borne pVIII on VMNSCs allows the clusters to mimic phage particles and target and enter MSCs to achieve gene delivery. The successful transfection of MSCs using VMSNCs is visualized by green fluorescence from enhanced green fluorescence protein (eGFP).

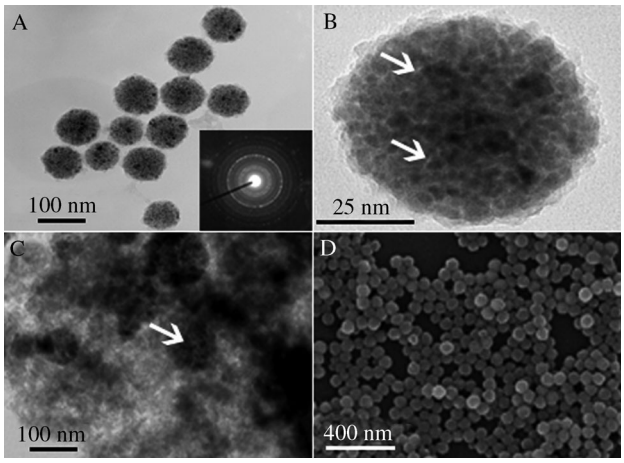

Figure 2. MSNCs synthesis. A) TEM image of MSNCs showing the magnetic NPs embedded in silica. Inset: electron diffraction pattern indicating the presence of Fe_3O_4 in MSNCs. B) High-magnification image of an individual nanocluster to show the intrinsic pores inside the cluster (pointed with arrows). C) TEM image of GSH-treated MSNCs, which shows the clusters were dissociated due to the cleavage of S–S bonds between the NPs inside nanoclusters. White arrows indicate the partially dissociated nanoclusters. D) Scanning electron microscope (SEM) image of MSNCs to show the large view and spherical morphology of clusters.

These GSH-cleavable MSNCs were formed by in situ hydrolysis of TEOS and MPTS in the presence of hydrophobic SPIO NPs dispersed in CTAB at 70 °C for 1 h. The excess CTAB present in the reaction medium was completely removed by centrifugation at 10000 rpm for 10 min for three times and resuspended in nanopure water. After complete removal of CTAB, the NPs solution was aged for 48 h, which resulted in the formation of approximately 80–100 nm spherical magnetic silica nanoclusters (MSNCs; Figure 2 A,B,D; Supporting Information, Figures S1–S3). Transmission electron microscopy (TEM) images (Figure 2 A,B) clearly verify that the magnetic NPs were embedded in a silica matrix to form a nanocluster.

During the in situ hydrolysis of TEOS and MPTS in the presence of hydrophobic SPIO NPs, upon aerial oxidation, S–S bonding between the formed thiolated silica NPs drives them to aggregate into clusters while the hydrophobic SPIO NPs are being embedded inside the resultant nanoclusters. The interparticle S–S bonding in the nanoclusters is confirmed by the fact that incubating the nanoclusters (10 nM) in 5 mM GSH for 4 h at 37 °C dissociated the nanoclusters into isolated NPs (Figure 2 C). TEM images (Figure 2 A,C) clearly show the difference between before and after GSH treatment, which confirms the presence of S–S bonding and subsequent cleavage upon GSH reduction. The intracellular GSH concentration is within the range of 1-10 mM,[9] thus allowing the use of GSH to trigger controlled intracellular release of cargo from disulfide-bonded nanoclusters owing to the cleavage of S–S bonds.

Magnetic measurement at 300 K using a superconducting quantum interference device (SQUID) magnetometer[10] shows that both SPIO NPs and MSNCs are superparamagnetic (Figure 3). However, the paramagnetic strength of MSNCs is determined to be 4.0 emu g^{-1} at 1.0 T, which is smaller than SPIO NPs by a factor of ten. This is mainly due to the weight percentage of SPIO NPs present in MSNCs. The magnetic measurement confirmed the superparamagnetic nature of our nanoclusters, which is crucial for magnetically guide the delivery of the gene-loaded nanoclusters into cells (magnetofection).

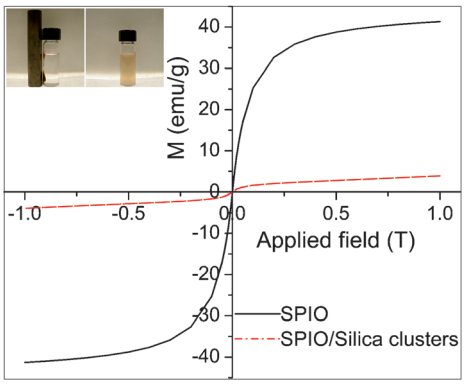

Figure 3. Hysteresis loops of SPIO NPs (straight black line) and cleavable MSNCs (dotted red line) measured by SQUID. Inset: photographs of the MSNCs in water with (left) and without (right) a magnet.

The DNA loading capability of the MSNCs before modification with PEI was estimated by gel electrophoresis. DNA was completely encapsulated when the mass ratio between nanoclusters and DNA reaches 1:1 (Supporting Information, Figure S4). Thus this ratio was used in the subsequent experiments. These MSNCs were further modified with PEI (MW = 8 kDa) and characterized by FTIR spectroscopy. The FTIR spectrum (Supporting Information, Figure S1) confirms the presence of PEI, SiO_2, and Fe_3O_4 in the nanoclusters. The zeta potential of the PEI modified MSNCs was determined to be $+26 \pm 2$ mV, which will promote the efficient gene transfection.

The pVIII was isolated from the MSC-targeting filamentous fd-tet phage, which was identified by us recently and had about 3900 copies of MSC-homing pVIII,[7] by phenol extraction following a reported procedure.[8] The MSC-homing pVIII purified from the MSC-targeting phage can favor the MSC-homing of the NPs modified with the pVIII. Towards this end, the isolated pVIII was conjugated to the PEI on the surface of the nanoclusters so that the nanoclusters can home to MSCs (Figure 1). Bioconjugation between the C-terminal end of pVIII and $-NH_2$ in PEI was carried out using a 1-ethyl-3-(3-dimethylaminopropyl)carbodiimide hydrochloride and N-hydroxysuccinimide (EDC/NHS) conjugation reaction. The resultant VMSNCs exhibited both magnetic and fusogenic properties.

A DTNB assay[11] was used to measure the concentration of thiol groups present in NPs formed owing to the cleavage of VMSNCs in the presence of GSH with a concentration of 1 mM or 0.1 mM (Supporting Information, Figure S5). The addition of GSH triggered the cleavage of disulfide bond in the nanoclusters and the concurrent formation of free thiol groups (Supporting Information, Figure S5), suggesting that thiol-fused MSNCs can be used as molecular switches for triggered release of therapeutics in cytoplasm by reducing the interparticle disulfide bonding in the presence of GSH available in the living cells (Scheme 1).

We later examined DNA release from VMSNCs in the presence and absence of GSH at a physiological concentration (1 mM; Supporting Information, Figure S6). Our data shows that GSH-treated VMSNCs demonstrated sustained release of DNA whereas the VMSNCs almost did not release DNA in the absence of GSH. These results suggest that GSH at an intracellular concentration can cleave the disulfide bond in the VMSNCs and consequently lead to the release of DNA from the nanoclusters (Scheme 1).

A 3-(4,5-dimethylthiazol-2-yl)-2,5-diphenyltetrazolium bromide (MTT) assay was then used to evaluate cytotoxicity at different concentrations of VMSNCs. At a concentration of 20 $\mu g\,mL^{-1}$, VMSNCs still showed high cell viability (around 96%; Figure 4). However, Lipofectamine 2000, the commercially available transfection reagent, at the same concentration showed less than 70% cell viability (Supporting Information, Figure S7). This fact shows that VMSCNs are more biocompatible than Lipofectamine 2000.

After the successful synthesis of desired VMSNCs with low toxicity, high gene-loading capability, and sufficient superparamagnetism, we conducted cell internalization studies in MSCs (Figure 5). The VMSNCs with FITC-labeled

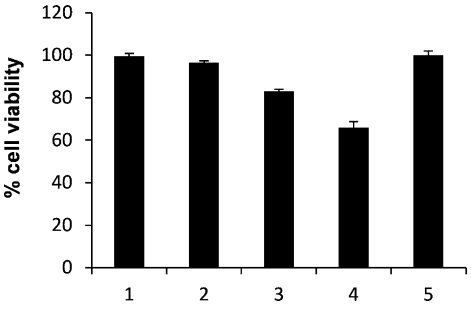

Figure 4. Cell viability studies by MTT assay of MSCs at different concentrations of VMSNCs. Bars 1 to 4 show the viability of MSCs with 10, 20, 40, and 80 $\mu g\,mL^{-1}$ of nanoclusters in 500 μL of fetal bovine serum (FBS) free Dulbecco's modified eagle medium (DMEM) incubated for 4 h, respectively. Bar 5 is the viability of control cells (without interacting with VMSNCs).

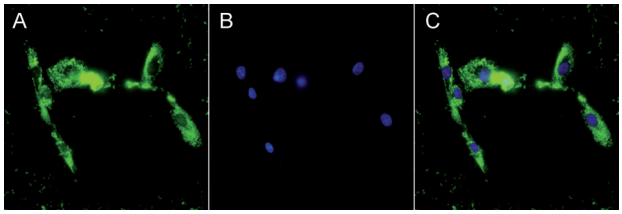

Figure 5. Internalization studies of VMSNCs carrying a green dye-labeled DNA. All images were captured at 40× optical zoom. A) Green fluorescence of FITC-labeled DNA entrapped in nanoclusters after interaction with MSCs to confirm the cell internalization capabilities of VMSNCs. B) DAPI-stained MSCs to show the cell nuclei. C) Merged image of A and B.

DNA loaded were incubated with MSCs at 37 °C. After incubation for 2 h, the cells were washed three times with PBS. Green fluorescence images (Figure 5) confirm that the VMSNCs were successfully internalized in MSCs. Our previous studies showed that a pVIII with cell-targeting peptide fused to its N-terminal could facilitate the cell-internalization of phage particles that bear the same pVIII.[12] Thus the internalization of VMSNCs in MSCs might be promoted by the MSC-homing pVIII on the surface of VMSNCs, which would facilitate the delivery of gene to MSCs.

The VMSNCs containing eGFP-VEGF plasmid and cell-targeting pVIII were dispersed in DMEM to transfect the MSCs in vitro. After 24 h of incubation, eGFP-VEGF gene was successfully delivered to MSCs by VMSNCs and expressed (Figure 6; Supporting Information, Figure S8). The gene expression was visualized with the reporter eGFP gene expression by green fluorescence (Supporting Information, Figure S8). The corresponding quantitative eGFP expression was evaluated by flow cytometry to determine the transfection efficiency (Figure 6) of VMSNCs at different transfection conditions (with or without pVIII or magnetic field) using Lipofectamine 2000 as a control. The transfection efficiency of our novel cleavable VMSNCs in the absence of magnetic field (25.80%) was significantly higher than that of the commercially available transfection reagent (Lipofect-

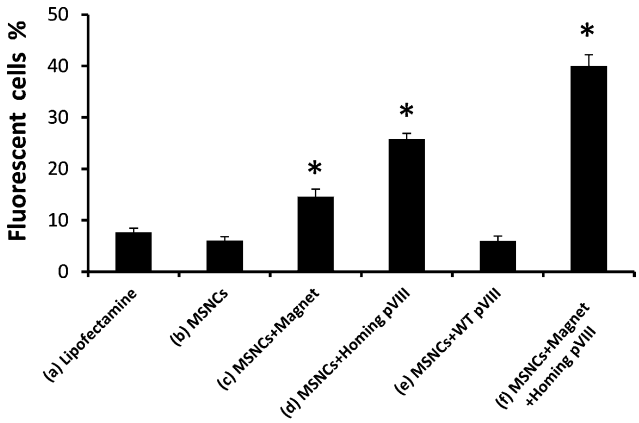

Figure 6. The efficiency of eGFP-VEGF gene transfection in MSCs by VMSNCs and control vectors. a) Transfection with Lipofectamine 2000. b) Transfection with MSNCs (that is, the nanoclusters without pVIII on the surface) in the absence of magnetic field. c) Transfection with MSNCs under 1T magnetic field. d) The VMSNCs (that is, MSNCs with MSC-homing pVIII) in the absence of a magnetic field. e) The VMSNCs with MSC-homing pVIII replaced by wild-type phage pVIII and in the absence of a magnetic field. f) The VMSNCs under 1 T magnetic field. Data are shown as mean ± SD ($n = 3$). Asterisk denotes $p < 0.01$ with Lipofectamine 2000 as a reference.

amine 2000; 7.66%). VMSNCs in the presence of magnetic field (1.0 Tesla) shows the highest level of transfection (40.01%) in comparison with VMSNCs in the absence of magnetic field (25.80%), MSNCs in the presence of magnetic field (14.64%), and MSNCs alone (6.05%). When MSNCs without any protein or with wild-type pVIII modified are used as a vector, the transfection efficiency is very low (less than 10%) and similar to that of Lipofectamine 2000. Our results clearly indicate that both MSCs homing phage protein and magnetic field help the VMSNCs to carry the eGFP-VEGF gene into MSCs. At the same time, VMSNCs transfection efficiency in the absence of the magnetic field is lower than that in the presence of the magnet, which is possibly due to the faster internalization and lower endosomal DNA degradation in the presence of an external magnetic field.

In summary, we developed novel VMSNCs for gene delivery to MSCs. We transferred the MSC-targeting pVIII from phage to nanoclusters to enable cell internalization. These VMSNCs are ideal gene therapy vectors owing to their MSC-homing capability and controlled release at the target site. Even in the absence of the magnetic field, the VMSNCs can deliver a gene to MSCs at a higher efficiency than commercially available vectors. The dual nature of virus mimicking and superparamagnetism make these vectors an ideal tool for the magnetically guided targeted delivery and possibly an ideal contrast enhancement agent for the magnetic resonance imaging in future in vivo applications.

Experimental Section

VMSNCs synthesis: 1 mM of isolated MSC-targeting pVIII protein was conjugated to the NH_2 of PEI on the surface of the 1 nM MSNCs to obtain VMSNCs. Bio-conjugation was carried out by protecting the $-NH_2$ groups using 2 mM of tert-butyl carbamate (BOC) in THF/H_2O to stop the self-conjugation of pVIII. The −COOH groups present in pVIII protein were activated using EDC/NHS. Then the EDC/NHS-activated and BOC-protected pVIII protein was incubated with PEI-modified DNA-loaded MSNCs for 4 h at pH 8.0 to form an amide bond between PEI and pVIII. The acid-labile BOC protection was then removed by treating with trifluoroacetic acid, followed by centrifugation to separate the by-products from VMSNCs.

Received: February 7, 2013
Revised: May 27, 2013
Published online: August 28, 2013

Keywords: gene delivery · nanoparticles · phage display · stem cells · virus mimetics

[1] a) A. A. Kocher, M. D. Schuster, M. J. Szabolcs, S. Takuma, D. Burkhoff, J. Wang, S. Homma, N. M. Edwards, S. Itescu, *Nat. Med.* **2001**, *7*, 430–436; b) D. Woodbury, E. J. Schwarz, D. J. Prockop, I. B. Black, *J. Neurosci. Res.* **2000**, *61*, 364–370; c) C. P. Hofstetter, E. J. Schwarz, D. Hess, J. Widenfalk, A. El Manira, D. J. Prockop, L. Olson, *Proc. Natl. Acad. Sci. USA* **2002**, *99*, 2199–2204.

[2] F. M. Chen, M. Zhang, Z. F. Wu, *Biomaterials* **2010**, *31*, 6279–6308.

[3] a) L. Naldini, U. Blomer, P. Gallay, D. Ory, R. Mulligan, F. H. Gage, I. M. Verma, D. Trono, *Science* **1996**, *272*, 263–267; b) H. B. Xia, Q. W. Mao, H. L. Paulson, B. L. Davidson, *Nat. Biotechnol.* **2002**, *20*, 1006–1010; c) T. C. He, S. B. Zhou, L. T. da Costa, J. Yu, K. W. Kinzler, B. Vogelstein, *Proc. Natl. Acad. Sci. USA* **1998**, *95*, 2509–2514.

[4] a) J. Dobson, *Gene Ther.* **2006**, *13*, 283–287; b) S. Prabha, W. Z. Zhou, J. Panyam, V. Labhasetwar, *Int. J. Pharm.* **2002**, *244*, 105–115; c) M. C. Pedroso de Lima, S. Simoes, P. Pires, H. Faneca, N. Duzgunes, *Adv. Drug Delivery Rev.* **2001**, *47*, 277–294; d) L. Wasungu, D. Hoekstra, *J. Controlled Release* **2006**, *116*, 255–264; e) T. G. Park, J. H. Jeong, S. W. Kim, *Adv. Drug Delivery Rev.* **2006**, *58*, 467–486; f) J. A. Wieland, T. L. Houchin-Ray, L. D. Shea, *J. Controlled Release* **2007**, *120*, 233–241.

[5] a) C. Madeira, R. Mendes, S. Ribeiro, J. Boura, M. Aires-Barros, C. da Silva, J. Cabral, *J. Biomed. Biotechnol.* **2010**, 735349; b) K. Corsi, F. Chellat, L. H. Yahia, J. C. Fernandes, *Biomaterials* **2003**, *24*, 1255–1264; c) H. H. Ahn, J. H. Lee, K. S. Kim, J. Y. Lee, M. S. Kim, G. Khang, I. W. Lee, H. B. Lee, *Biomaterials* **2008**, *29*, 2415–2422; d) J. McMahon, S. Conroy, M. Lyons, U. Greiser, C. O'Shea, P. Strappe, L. Howard, M. Murphy, F. Barry, T. O'Brien, *Stem Cells Dev.* **2006**, *15*, 87–96.

[6] N. Gandra, G. Abbineni, X. Qu, Y. Huai, L. Wang, C. Mao, *Small* **2013**, *9*, 215–221.

[7] K. Ma, D.-D. Wang, Y. Lin, J. Wang, V. Petrenko, C. Mao, *Adv. Funct. Mater.* **2013**, *23*, 1172–1181.

[8] R. Knippers, H. Hoffmann-Berling, *J. Mol. Biol.* **1966**, *21*, 281–292.

[9] a) R. Hong, G. Han, J. M. Fernández, B.-j. Kim, N. S. Forbes, V. M. Rotello, *J. Am. Chem. Soc.* **2006**, *128*, 1078–1079; b) R. Cheng, F. Feng, F. Meng, C. Deng, J. Feijen, Z. Zhong, *J. Controlled Release* **2011**, *152*, 2–12.

[10] F. Y. Cheng, C. H. Su, Y. S. Yang, C. S. Yeh, C. Y. Tsai, C. L. Wu, M. T. Wu, D. B. Shieh, *Biomaterials* **2005**, *26*, 729–738.

[11] a) R. Y. Sweeney, C. Mao, X. Gao, J. L. Burt, A. M. Belcher, G. Georgiou, B. L. Iverson, *Chem. Biol.* **2004**, *11*, 1553–1559; b) G. L. Ellman, *Arch. Biochem. Biophys.* **1959**, *82*, 70–77.

[12] G. Abbineni, S. Modali, B. Safiejko-Mroczka, V. A. Petrenko, C. Mao, *Mol. Pharm.* **2010**, *7*, 1629–1642.

